Published in final edited form as:

J Alzheimers Dis. 2015 ; 48(3): 687–702. doi:10.3233/JAD-150298.

Identification of Novel Tau Interactions with Endoplasmic Reticulum Proteins in Alzheimer's Disease Brain

Shelby Meier[a], **Michelle Bell**[a], **Danielle N. Lyons**[a], **Alexandria Ingram**[a], **Jing Chen**[b], **John C. Gensel**[c,e], **Haining Zhu**[b], **Peter T. Nelson**[a,d], and **Jose F. Abisambra**[a,e,*]

[a]Sanders Brown Center on Aging, University of Kentucky, Lexington, KY, USA

[b]Department of Molecular and Cellular Biochemistry, University of Kentucky, Lexington, KY, USA

[c]Spinal Cord and Brain Injury Research Center, University of Kentucky, Lexington, KY, USA

[d]Department of Pathology, Division of Neuropathology, University of Kentucky, Lexington, KY, USA

[e]Department of Physiology, College of Medicine, University of Kentucky, Lexington, KY, USA

Abstract

Alzheimer's disease (AD) is a progressive neurodegenerative disorder that is pathologically characterized by the formation of extracellular amyloid plaques and intraneuronal tau tangles. We recently identified that tau associates with proteins known to participate in endoplasmic reticulum (ER)-associated degradation (ERAD); consequently, ERAD becomes dysfunctional and causes neurotoxicity. We hypothesized that tau associates with other ER proteins, and that this association could also lead to cellular dysfunction in AD. Portions of human AD and non-demented age matched control brains were fractionated to obtain microsomes, from which tau was co-immunoprecipitated. Samples from both conditions containing tau and its associated proteins were analyzed by mass spectrometry. In total, we identified 91 ER proteins that co-immunoprecipitated with tau; 15.4% were common between AD and control brains, and 42.9% only in the AD samples. The remainder, 41.8% of the proteins, was only seen in the control brain samples. We identified a variety of previously unreported interactions between tau and ER proteins. These proteins participate in over sixteen functional categories, the most abundant being involved in RNA translation. We then determined that association of tau with these ER proteins was different between the AD and control samples. We found that tau associated equally with the ribosomal protein L28 but more robustly with the ribosomal protein P0. These data suggest that the differential association between tau and ER proteins in disease could reveal the pathogenic processes by which tau induces cellular dysfunction.

[*]Correspondence to: Jose F. Abisambra, Sanders-Brown Center on Aging and Department of Physiology, College of Medicine, University of Kentucky, 800 S Limestone Street, Lexington, KY 40536-0230, USA. Tel.: +1 859 218 3852; ; Email: joe.abisambra@uky.edu

Authors' disclosures available online (http://j-alz.com/manuscript-disclosures/15-0298r2).

Keywords

Alzheimer's disease; co-immunoprecipitation; endoplasmic reticulum; mass spectrometry; microsome; ribosome; tau; tauopathies

INTRODUCTION

Alzheimer's disease (AD) is a progressive neurodegenerative disorder that affects 5.2 million Americans [1] and 36 million people worldwide [2]. This number is expected to rise to 13.8 million by 2050. The direct and indirect costs of maintaining the quality of life of AD amounts to $203 billion annually. Since there is currently no cure for AD, and therapeutic interventions are ineffective in preventing the dramatic rise of patients, expenditures are projected to reach $1.2 trillion annually by 2050.

The pathological hallmarks of AD consist of amyloid plaques and neurofibrillary tangles (NFTs). Plaques result from extracellular aggregation of a 40–42 amino acid peptide termed amyloid-β (Aβ) (reviewed in [3]). Meanwhile, NFTs are intraneuronal lesions comprised of aberrant aggregates of the microtubule-associated protein tau. Within NFTs, tau is abnormally folded, oligomerized, hyperphosphorylated, and mislocalized [4–6]. In AD, as well as in other tauopathies, tau becomes neurotoxic [7]; however, the exact mechanisms leading to tau neurotoxicity have not been identified.

As a microtubule stabilizing protein [8], tau interacts with various other proteins that are transported along microtubules. Pathogenic tau adopts a β-pleated sheet conformation [9], rendering it hydrophobic and able to bind non-specifically to other proteins and itself (reviewed in [10, 11]). In many cases, these aberrant linkages have deleterious consequences to the functions and processes in which tau-associated proteins participate [11–16]. For example, soluble, pathological tau conformers associate with endoplasmic reticulum (ER)-associated degradation (ERAD) proteins, and abrogate ERAD function [12].

Recent studies suggest that a key mechanism of neuronal dysfunction in neurodegenerative diseases is impaired protein synthesis [17]. This phenomenon could be the result of tau-mediated impairment of ribosomal function. Tau normally associates with ribosomes [18]. However, due to its intrinsically disordered conformation, which is amplified in disease, tau binds to proteins that participate in RNA translation thereby impairing translation [19]. Thusly, a mechanism of tau-mediated neurodegeneration could implicate aberrant tau-ribosomal interactions.

In the current study, we sought to identify tau-associated ER proteins with particular emphasis on proteins involved in RNA translation. We hypothesized that tau-associated ER proteins could serve as potential therapeutic targets. We identified tau-interacting ER proteins in both AD and non-AD brains with an integrated approach involving sub-cellular fractionation, co-immunoprecipitation, and mass spectrometry. We established three types of tau-associated ER proteins: those that were identified in AD brains, others that were only identified in non-AD brains, and those that were common to both. Interestingly, 85% of the proteins we identified had not been previously established as associating with tau. Among

them, were several proteins that participate in RNA translation. To validate our approach, we focused on the ribosomal proteins L28 and P0, which had not been previously identified to be associated with tau, and we found that tau associated more robustly with P0 in the AD brain. Overall, these data suggest that changes in the association between tau and ER proteins could underlie pathogenic mechanisms leading or contributing to cellular dysfunction evident in AD. Further characterization and validation of AD tau-associated ER proteins and their functions could lead to better understanding of the pathogenesis of AD and other tauopathies.

MATERIALS AND METHODS

Human brain samples

Samples were obtained from the University of Kentucky-Alzheimer's Disease Center Tissue Bank. All sample collection and experimental procedures involving human subjects were in compliance with the University of Kentucky Institutional Review board (IRB) protocols. Samples from the superior and mid-temporal gyrus (Brodmann areas 21/22) were used. AD tissues were from symptomatic individuals and they were neuropathologically scored as Braak V (female, 93 years old), VI (male, 88 years old), and VI (female, 80 years old); non-demented control samples were scored Braak I (male, 79 years old), II (female, 94 years old), and II (female, 88 years old). The average postmortem interval (between death and the tissue being snap-frozen in liquid nitrogen) was 3.0 h.

Microsome isolation

Microsomes were isolated as previously described [20, 21] and modified for brain [22]. Briefly, 200 mg of human brain samples were dounce homogenized in 0.25 M sucrose containing 1X protease inhibitor mixture (Calbiochem), 100 mM phenylmethylsulfonyl fluoride, and 1X phosphatase inhibitor II and III cocktails (Sigma). All samples were then centrifuged at 16,000 × g for 15 min at 4°C. The supernatant was transferred and centrifuged at 100,000 × g for 1 h at 4°C. The pellet, which corresponded to the microsomal protein fraction, was resuspended in RIPA buffer containing 1X protease inhibitor mixture (Calbiochem), 100 mM phenylmethylsulfonyl fluoride, and 1X phosphatase inhibitor II and III cocktails (Sigma).

Co-immunoprecipitations (co-IP) and western blotting

Co-IP was performed as previously described [23] using antibodies for tau (Tau5 EMD Millipore), actin (Sigma-Aldrich), RPL28 (GeneTex), or RPP0 (Gene-Tex). Western blots were performed as previously described [24]. Briefly, 20 μg of protein were denatured by mixing with a sample buffer (consisting of 2x Laemmli buffer with 5% β-mercaptoethanol) and subjecting to heat at 100°C for 10 min. Samples were loaded in 10% tris-glycine gels (Life Technologies). Gels were subjected to 100 mV until the dye front reached the bottom of the gel. We then performed wet transfers as indicated previously [25]. Samples were blocked in 7% non-fat dry milk (LabScientific) with 0.02% sodium azide. This milk was used to mix antibodies for incubation with the membranes. Antibodies used were anti total tau h-150 (1:1000) from Santa Cruz Biotechnology, actin (1:1000) from Sigma, RPL28 from GeneTex, RPP0 from GeneTex, and calnexin C-20 from Santa Cruz Biotechnology.

Immunofluorescence

Frozen brain samples were fixed in 4% paraformaldehyde. Fixed brains were cryoprotected in successive 24 h increments of 10%, 20%, and 30% sucrose gradients as described previously [26]. Brains were frozen on a temperature-controlled freezing stage, sectioned (25 μm) on a sliding microtome, and stored in a solution of PBS containing 0.02% sodium azide at 4°C. Immunostaining was performed following protocols described previously with minor modifications [22]. Brain sections were mounted on glass slides with medium (30% ethanol in PBS). Once dry, sections were blocked and permeabilized in blocking buffer (4% normal goat serum, 0.2% Triton X-100, and 0.02% sodium azide in TBS) for 1 h. Slides were incubated overnight at 4°C with the following antibodies: tau h-150 (1:50), PHF1 (1:50), calnexin C-20 (1:50), calnexin F-17 (1–50). Slides were then washed with TBS and incubated with Alexa Fluor 488 nm and Alexa Fluor 594 nm secondary antibodies (Life Technologies) at 1:2000 for 2 h at room temperature. Tissues were stained with Sudan black to block autofluorescence inherent to the sample. Slides were then washed again and incubated with Neurotrace (1:200) according to the manufacturer's recommendations. Slides with both AD and control were stained omitting primary antibodies in order to identify non-specific background signal.

Microscopy

All slides were imaged using a Nikon Eclipse Ti laser-scanning confocal microscope. Fields for colocalization analysis were randomly selected based upon tau immunolabeling by an investigator blinded to group inclusion. Specifically, fields were chosen that included areas of tau staining with morphological distribution in agreement with NeuN labeling; ER labeling was not considered in field selection. All immunolabeling acquisition intensities, field sizes, and microscopy settings were kept consistent across all images. Scatter plots and images for graphical representation of co-localization were prepared using the NIS Elements 4.20 (Nikon) and Photoshop Cs6 (Adobe) software programs and were based upon cells that most closely approximated the group means.

Co-localization analysis

Images were analyzed for co-localization as previously described with minor modifications [12]. Briefly, regions of interest (ROIs) corresponding to z-stack images of neurons that stained positively for calnexin and tau (either total tau or PHF1) were selected for co-localization analysis. Three to five ROIs were selected per image, and there were at least three images per brain from three AD brains. Z-stack images were analyzed according to [27] using Pearson's, Manders', and Costes' (auto-threshold and randomization control) coefficients.

Mass spectrometry (MS) and proteomics data analysis

Each lane in the gel was excised into 12 major portions and subjected to dithiothreitol reduction, iodoacetamide alkylation, and in-gel trypsin digestion using a standard protocol as previously reported [28, 29]. The resulting tryptic peptides were extracted, concentrated to 15 μl each using a SpeedVac, and 5 μl was injected for nano-LC-MS/MS analysis. LC-MS/MS data were acquired on an LTQ Velos Orbitrap mass spectrometer (Thermo Fisher

Scientific, Waltham, MA) coupled with a Nano-LC Ultra/cHiPLC-nanoflex HPLC system (Eksigent, Dublin, CA) through a nano-electrospray ionization source. The tryptic peptides sample was injected by an autosampler, desalted on a trap column, and subsequently separated by reverse phase C18 column (75 mm i.d. × 150 mm) at a flow rate of 250 nL/min. The HPLC gradient was linear from 5% to 60% mobile phase B for 30 min using mobile phase A (H_2O, 0.1% formic acid) and mobile B (90% acetonitrile, 0.1% formic acid). Eluted peptides were analyzed using data-dependent acquisition: peptide mass spectrometry was obtained by Orbitrap with a resolution of 60,000. The seven most abundant peptides were subjected to collision induced dissociation and MS/MS analysis in LTQ linear trap. The LC-MS/MS data were submitted to a local MASCOT server for MS/MS protein identification search via the ProteomeDiscoverer software. The mass error tolerance was 5 ppm for peptide MS and 0.8 Da for MS/MS. All peptides were required to have an ion score greater than 30 ($p < 0.05$). The false discovery rate in each LC-MS/MS analysis was set to be less than 1%. Proteins that were identified in the actin-IP samples were excluded from the tau-IP list. Although tau binds to actin under normal conditions this interaction occurs primarily in the growth cone [30]. Since tau tangles deposit in the soma [31], our results reflect primarily ER proteins associated with pathological tau [32].

Functional categorization of MS results

Functional descriptions for all proteins were acquired by searching for accession numbers in the UNIPROT database (http://www.uniprot.org). Proteins were categorized by function (Fig. 3B). In some cases, proteins were multifunctional, but they were only organized into one parameter as justified by their primary function.

Western blot analysis

For western blots, the relative intensity of the bands was measured using ImageJ. Bands of the protein of interest were normalized to a loading control. Statistical analysis of the bands was performed using Student's *t*-test. All graphs were prepared in Prism 6 (GraphPad).

RESULTS

Tau abnormally associates with proteins on the cytosolic surface of the ER in the rTg4510 tau transgenic model [12]. VCP and Hrd1 are two examples of tau-associated ER proteins, and both of these proteins play crucial roles in ERAD. As a result of this abnormal interaction, ERAD function becomes impaired in tau transgenic mice and in AD brain. Therefore, we hypothesized that tau associated with other ER proteins, the functions of which could similarly be altered by the abnormal association with tau.

In AD brains, tau tangle formation occurs primarily in neuronal soma [31, 33]. In fact, a large pool of tau deposits in the perinuclear region coincident with the ER [12, 34, 35]. To further characterize this interaction, we performed subcellular fractionation of three AD and three age-matched, non-demented control brains to isolate the microsomal compartment, which is predominantly composed of ER and associated proteins [36]. Tau formed high molecular weight complexes (Fig. 1A, C) in AD brains which is characteristic of hyperphosphorylated and detergent insoluble pathological tau (reviewed in [37]).

Conversely, control brains showed a typical tau smear between 48–60 kDa. We quantified the amount of tau in the 48–60 kDa range of AD and control whole brain lysates and microsomes. We determined that while tau levels did not differ between whole cell lysates of AD and control, AD microsomes contained 34% more tau than control (Fig. 1A–1D). These data suggest that tau shifts in tau distribution in AD. We then performed co-immunofluorescent staining of human AD and control brains to determine the distribution of total and hyperphosphorylated tau with the ER (Fig. 1E, L). We co-immunofluorescently labeled total tau or hyperphosphorylated tau (pS396/S404 detected with PHF1) and calnexin, an ER transmembrane protein [38]. We found that both tau and hyperphosphorylated tau decorated the ER by largely co-localizing with calnexin (Fig. 1G, K).

To reveal the identity of tau-associated ER proteins, we isolated microsomes from human AD and control brains and performed co-immunoprecipitation analyses using an anti-tau antibody (Tau5); actin was co-immunoprecipitated from the same tissues as a control. All samples were processed for liquid chromatography-tandem mass spectrometry (LC-MS/MS) (Fig. 2).

We applied robust exclusion criteria to minimize false positive results. First, each peptide matched from a MS/MS spectrum had an ion score based on the calculated probability, p, that the observed match between the experimental data and the database sequence was a random event. We set an ion score threshold to achieve $p < 0.05$. The scores in the tables (Protein Score) were mathematically derived from the ion scores of all peptides matched to this protein. Confidence in protein identification is directly proportional to the magnitude of the Protein Score. In addition, we set the false discovery rate at 1% for the MASCOT data analysis to ensure the high confidence of all proteins identified from the LC-MS/MS data. Second, proteins that were identified in the actin-IP samples were excluded from the tau-IP list. Although tau binds to actin under normal conditions this interaction occurs primarily in the growth cone [30]. Since tau tangles deposit in the soma [31], our results reflect primarily ER proteins associated with pathological tau [32].

Data were submitted to a local Mascot server for protein identification analysis. Tau was identified in both the AD and non-AD samples, indicating that the co-immunoprecipitation was successful. In addition, a total of 92 proteins were identified (Tables 1–3). Of these, 39 (42.4%) were found in AD brain (Table 1), 38 (41.3%) were only found in the non-AD brain (Table 2), and 15 (16.3%) were found in both AD and non-AD (Table 3; Fig. 3A). Interestingly, 77 of these (85%) had not been previously identified as tau-interacting proteins. Based on previous work showing that the aberrant association of tau with ERAD proteins caused ERAD impairments [12], we grouped the 92 proteins identified in our screen by functional categories (Fig. 3B). Each protein was assigned a function based on the description in the UNIPROT database. Figure 3B represents the relative abundance of proteins from each category.

Our screen showed that the ribosomal proteins L28 and P0 co-immunoprecipitated differentially with tau in both AD and control brains. More specifically, P0 did not complex with tau in control brains. To confirm these results, we co-immunoprecipitated L28 or P0 from human AD or control brain microsomes. We determined that tau formed a complex

with both L28 and P0 (Fig. 4A, B); however, the tau-P0 association was much more robust in the AD microsomes than in control, as suggested by the MS/MS data (Fig. 4C). Interestingly, the data show that P0 formed a complex with high molecular weight tau species. We also performed the reverse co-immunoprecipitation by isolating tau from AD and control microsomes and measuring the levels of P0 and L28 by western blot. We found no significant difference in the levels of P0 or L28 in the reverse co-immunoprecipitation (Fig. 4G). The input blot shows that the primary tau species that was isolated corresponded to a 50–60kDa tau band that lacks post-translational modifications. These data suggest that P0 and L28 associate normally with tau around the ER; however, in AD brains, there is a significant increase in the association of high molecular weight tau (heavily post-translationally modified and pathological) with P0.

DISCUSSION

We present a list of 92 tau-associated ER proteins. The list contains proteins that have been previously identified as disease modulators such as AD-related tau kinases and apolipoprotein E (ApoE). However, 77 proteins (85%) have not been previously linked to tau. Among the identified proteins were several that participate in ERAD thereby validating this approach with previous findings [12]. Moreover, we show that the subcellular fractionation-coIP-MS/MS approach is sufficiently sensitive to identify different affinities of tau for L28 and P0, which are closely localized in ribosomes.

The newly identified tau-associated ER proteins could reveal tau functions that have not been previously described. For instance, synaptojanin, a protein involved in the uncoating of synaptic vesicles [39], was identified as a tau-associated ER protein in normal, non-AD brain. This suggests that tau facilitates synaptojanin's function and therefore indirectly participates in endocytic processes for synaptic function. Similarly, loss of the tau-synaptojanin interaction would reduce uncoating of synaptic vesicles altering synaptic function; indeed, synaptojanin was not identified as a tau-associated ER protein in the AD brain data set. Another example is caspase-14, which had not been previously identified as a tau interacting protein but was a positive hit in the normal brain. This could be the first evidence of tau cleavage by another caspase besides caspases 3, 6, 7, 8, and 9 [40–43]. Since this association was not determined in the AD brain, it is possible that caspase-14 function is beneficial, and loss of the interaction could lead to early pathogenesis.

Ribosomal proteins constituted the largest functional category of tau-associated ER proteins. Yet, since the immunoprecipitation was performed with Tau5, an antibody that binds to the middle region of tau (aa 210–241), it is possible that the co-IP isolated both mature and nascent tau (partially translated tau beyond aa 241), the latter of which could still be attached to ribosomes while it is being translated. Identification of chaperones as tau-associated ER proteins also supports the idea that this is non-pathological nascent tau. However, some of these tau-associated ribosomal proteins are different between the AD and control brains. For instance, ribosomal proteins P0 and L28 showed differential association with pathological tau suggesting possible disease-based differences that could alter ribosomal function. Indeed, hyperphosphorylated tau associates with ribosomes in AD and tauopathy models but not in normal models but the consequences of this interaction are unknown [19, 44]. This is

critical to understand disease mechanisms since ribosomal dysfunction has been associated with AD pathogenesis [45]. Ribosomal proteins P0 and L28 are both structural proteins located in the 60 S subunit. While the individual proteins have not been studied in depth, the function of the 60 S subunit has been extensively covered. Proteins in this subunit participate in ribosome biogenesis, all phases of translation, viral transcription, and nonsense-mediated decay of mRNA [46]. The structural proteins in the 60 S ribosomal subunit play a critical part in joining the 60 S subunit with the 40 S subunit. Since P0 and L28 are structural proteins, it is possible that the association of abnormal tau with these proteins could prevent the coupling of the 60 S subunit with the 40 S subunit and would subsequently lead to a decrease in translation.

Our study further characterizes region-specific features of previously identified tau-interacting proteins. For instance, ApoE, the main cholesterol transporter in the brain, was previously identified as a tau-interacting protein [47]. Since expression of different ApoE iso-forms confer either increased risk for AD (ApoE4) or protection from AD (ApoE2), and tau is intricately involved in AD pathology, the ApoE-tau relationship should be studied in further detail. Identification of ApoE in our study highlights that this interaction occurs in proximity to the ER. Interestingly, ApoE was identified as a tau-associated ER protein in both AD and non-AD brains. Therefore, the ApoE-tau interaction plays a normal role in the brain, and aberrancy of the interaction could be a component of the AD mechanism.

Spectrin, a cytoskeletal protein that was identified in our screen, had also been reported to associate with tau [48]. However, the association occurs as a consequence of disease or trauma instead of a direct interaction [49, 50]. In AD and traumatic brain injury, axonal damage activates calpains and caspases that cleave tau and spectrin. Consequently, cleaved tau and spectrin levels increase in parenchyma and cerebrospinal fluid [37]. These cleavage products have been studied as potential biomarkers of AD diagnosis and traumatic brain injury severity.

The association of a functional category with tau is more robust than that of tau with an individual protein. Therefore, while Table 1 presents interesting leads, Figure 3B offers tantalizing support for unidentified tau functions, the disturbance of which could be linked to AD. For example, identification of complement C3 as a tau-associated ER protein is insufficient evidence to suggest involvement of tau in regulating inflammatory processes. However, identification of other proteins that participate in inflammation, such as S100A8, S100A9, and inter-alpha-trypsin inhibitor as tau-associated ER proteins, supports the possibility of a role for tau in inflammation.

Although the mass spectrometry platform maximizes the sample input and yields a high amount of data, it is limited in the characterization of protein-protein interactions. Therefore, identification of individual tau partners must be validated to establish whether both proteins associate or interact. Albeit, despite the robust exclusion criteria we applied to our data, we identified tau-associated ER proteins that were previously validated as tau-interacting proteins such as ApoE and annexin, among others (Table 1) [8, 47, 51]. Tubulin, which interacts with both tau and actin, was identified in both co-immunoprecipitates. Since our exclusion criterion to limit false positives involved eliminating proteins identified in the

actin co-IP from the tau co-IP, we excluded tubulin from the list of tau-interacting proteins. Our approach adds novelty to these findings by establishing that this interaction might occur in brain microsomes.

We utilized robust exclusion criteria that showed no association between tau and the ribosomal protein P0 in non-demented control brain. Further characterization of these interactions revealed that tau indeed associated with P0 in both the AD and control samples; these data suggest that the exclusion criteria considered the less robust tau-P0 association below the threshold of a true positive hit. Furthermore, these data underscore the importance of validating MS/MS results such as the tau-ER proteins identified herein.

AD is a complex disease that often presents other clinical and pathological signs. Considering the complexity of AD etiology, it is possible that our current results are not unique to AD. In fact, they could be a common occurrence in many and newly-characterized tauopathies [52].

In conclusion, we performed a selective identification of ER proteins that associate with tau in AD and control brains. Further characterization of the dynamic changes in the association of tau and the listed proteins could reveal novel insights into the pathogenesis and progression of AD and related tauopathies. In addition, the tau-associated ER proteins in non-AD brain could identify tau functions that have not been previously described. Future efforts involve biochemical validation of these tau-associated ER proteins as tau-interacting proteins, characterization of the role of normal tau in the functional categories (Fig. 3B), and determination of the impact of pathological tau on the function of the tau-associated ER proteins in AD brain.

Acknowledgments

We acknowledge the University of Kentucky Alzheimer's Disease Center (UK-ADC) and its Neuropathology Core NIH/NIA, which is supported by NIH/NIA P30 AG028383. We also acknowledge the University of Kentucky Proteomics Core that is partially supported by grants from the NIH/NIGMS (P20GM103486) and the NIH/NCI (P30CA177558). This work was also supported in part by NIH R01NS077284 (to H.Z.). The LC-MS/MS instrument was acquired with a High-End Instrumentation Grant S10RR029127 (to H.Z.) from the NIH. We further acknowledge NIH/NINDS P30NS051220 for support and maintenance of the microscopy core used for imaging. J.F.A., D.L., and S.M. were supported by the Alzheimer's Association NIRG-14-322441, NIH/NIMHD LRP, UK Center for Clinical and Translational Science Pilot Award supported by NIH/NCATS 5UL1TR000117-04, UK-ADC Pilot Award 8.1 supported by NIH/NIA P30 AG028383, and the UK Epilepsy Center Pilot Project. We thank Dr. Peter Davies for his generous contribution of the PHF1 antibody used for immunofluorescent staining. We thank Ms. Ela Patel and Ms. Sonya Anderson with their assistance accessing the human brain tissue. We also thank Ms. Linda Simmerman for her technical assistance with microscopy. Finally, we thank Maria Bodero for her contributions to these studies.

References

1. Alzheimer's Association. 2014 Alzheimer's disease facts and figures. Alzheimers Dement. 2014; 10:e47–e92. [PubMed: 24818261]
2. Prince M, Bryce R, Albanese E, Wimo A, Ribeiro W, Ferri CP. The global prevalence of dementia: A systematic review and metaanalysis. Alzheimers Dement. 2013; 9:63–75. e62. [PubMed: 23305823]
3. Murphy MP, LeVine H 3rd. Alzheimer's disease and the amyloid-beta peptide. J Alzheimers Dis. 2010; 19:311–323. [PubMed: 20061647]

4. Grundke-Iqbal I, Iqbal K, Tung YC, Quinlan M, Wisniewski HM, Binder LI. Abnormal phosphorylation of the microtubule-associated protein tau (tau) in Alzheimer cytoskeletal pathology. Proc Natl Acad Sci U S A. 1986; 83:4913–4917. [PubMed: 3088567]
5. Lasagna-Reeves CA, Castillo-Carranza DL, Sengupta U, Guerrero-Munoz MJ, Kiritoshi T, Neugebauer V, Jackson GR, Kayed R. Alzheimer brain-derived tau oligomers propagate pathology from endogenous tau. Sci Rep. 2012; 2:700. [PubMed: 23050084]
6. Takashima A. Tauopathies and tau oligomers. J Alzheimers Dis. 2013; 37:565–568. [PubMed: 23948895]
7. Lasagna-Reeves CA, Castillo-Carranza DL, Sengupta U, Clos AL, Jackson GR, Kayed R. Tau oligomers impair memory and induce synaptic and mitochondrial dysfunction in wild-type mice. Mol Neurodegener. 2011; 6:39. [PubMed: 21645391]
8. Weingarten MD, Lockwood AH, Hwo SY, Kirschner MW. A protein factor essential for microtubule assembly. Proc Natl Acad Sci U S A. 1975; 72:1858–1862. [PubMed: 1057175]
9. von Bergen M, Friedhoff P, Biernat J, Heberle J, Mandelkow EM, Mandelkow E. Assembly of tau protein into Alzheimer paired helical filaments depends on a local sequence motif ((306)VQIVYK(311)) forming beta structure. Proc Natl Acad Sci U S A. 2000; 97:5129–5134. [PubMed: 10805776]
10. Mandelkow EM, Mandelkow E. Biochemistry and cell biology of tau protein in neurofibrillary degeneration. Cold Spring Harb Perspect Med. 2012; 2:a006247. [PubMed: 22762014]
11. Abisambra JF, Jinwal UK, Jones JR, Blair LJ, Koren J 3rd, Dickey CA. Exploiting the diversity of the heat-shock protein family for primary and secondary tauopathy therapeutics. Curr Neuropharmacol. 2011; 9:623–631. [PubMed: 22654720]
12. Abisambra JF, Jinwal UK, Blair LJ, O'Leary JC 3rd, Li Q, Brady S, Wang L, Guidi CE, Zhang B, Nordhues BA, Cockman M, Suntharalingham A, Li P, Jin Y, Atkins CA, Dickey CA. Tau accumulation activates the unfolded protein response by impairing endoplasmic reticulum-associated degradation. J Neurosci. 2013; 33:9498–9507. [PubMed: 23719816]
13. Abisambra JF, Blair LJ, Hill SE, Jones JR, Kraft C, Rogers J, Koren J 3rd, Jinwal UK, Lawson L, Johnson AG, Wilcock D, O'Leary JC, Jansen-West K, Muschol M, Golde TE, Weeber EJ, Banko J, Dickey CA. Phosphorylation dynamics regulate Hsp27-mediated rescue of neuronal plasticity deficits in tau transgenic mice. J Neurosci. 2010; 30:15374–15382. [PubMed: 21084594]
14. Abisambra JF, Jinwal UK, Suntharalingam A, Arulselvam K, Brady S, Cockman M, Jin Y, Zhang B, Dickey CA. DnaJA1 antagonizes constitutive Hsp70-mediated stabilization of tau. J Mol Biol. 2012; 421:653–661. [PubMed: 22343013]
15. Dickey CA, Kamal A, Lundgren K, Klosak N, Bailey RM, Dunmore J, Ash P, Shoraka S, Zlatkovic J, Eckman CB, Patterson C, Dickson DW, Nahman NS Jr, Hutton M, Burrows F, Petrucelli L. The high-affinity HSP90-CHIP complex recognizes and selectively degrades phosphorylated tau client proteins. J Clin Invest. 2007; 117:648–658. [PubMed: 17304350]
16. Jinwal UK, Akoury E, Abisambra JF, O'Leary JC 3rd, Thompson AD, Blair LJ, Jin Y, Bacon J, Nordhues BA, Cockman M, Zhang J, Li P, Zhang B, Borysov S, Uversky VN, Biernat J, Mandelkow E, Gestwicki JE, Zweckstetter M, Dickey CA. Imbalance of Hsp70 family variants fosters tau accumulation. FASEB J. 2013; 27:1450–1459. [PubMed: 23271055]
17. Moreno JA, Radford H, Peretti D, Steinert JR, Verity N, Martin MG, Halliday M, Morgan J, Dinsdale D, Ortori CA, Barrett DA, Tsaytler P, Bertolotti A, Willis AE, Bushell M, Mallucci GR. Sustained translational repression by eIF2alpha-P mediates prion neurodegeneration. Nature. 2012; 485:507–511. [PubMed: 22622579]
18. Papasozomenos SC, Binder LI. Phosphorylation determines two distinct species of Tau in the central nervous system. Cell Motil Cytoskeleton. 1987; 8:210–226. [PubMed: 2446784]
19. Nelson PT, Saper CB. Ultrastructure of neurofibrillary tangles in the cerebral cortex of sheep. Neurobiol Aging. 1995; 16:315–323. [PubMed: 7566341]
20. Ness GC, Sample CE, Smith M, Pendleton LC, Eichler DC. Characteristics of rat liver microsomal 3-hydroxy-3-methylglutaryl-coenzyme A reductase. Biochem J. 1986; 233:167–172. [PubMed: 3082322]

21. Lopez D, Abisambra Socarras JF, Bedi M, Ness GC. Activation of the hepatic LDL receptor promoter by thyroid hormone. Biochim Biophys Acta. 2007; 1771:1216–1225. [PubMed: 17572141]
22. Abisambra JF, Fiorelli T, Padmanabhan J, Neame P, Wefes I, Potter H. LDLR expression and localization are altered in mouse and human cell culture models of Alzheimer's disease. PLoS One. 2010; 5:e8556. [PubMed: 20049331]
23. Jinwal UK, Abisambra JF, Zhang J, Dharia S, O'Leary JC, Patel T, Braswell K, Jani T, Gestwicki JE, Dickey CA. Cdc37/Hsp90 protein complex disruption triggers an autophagic clearance cascade for TDP-43 protein. J Biol Chem. 2012; 287:24814–24820. [PubMed: 22674575]
24. Abisambra J, Jinwal UK, Miyata Y, Rogers J, Blair L, Li X, Seguin SP, Wang L, Jin Y, Bacon J, Brady S, Cockman M, Guidi C, Zhang J, Koren J, Young ZT, Atkins CA, Zhang B, Lawson LY, Weeber EJ, Brodsky JL, Gestwicki JE, Dickey CA. Allosteric heat shock protein 70 inhibitors rapidly rescue synaptic plasticity deficits by reducing aberrant tau. Biol Psychiatry. 2013; 74:367–374. [PubMed: 23607970]
25. Jones JR, Lebar MD, Jinwal UK, Abisambra JF, Koren J 3rd, Blair L, O'Leary JC, Davey Z, Trotter J, Johnson AG, Weeber E, Eckman CB, Baker BJ, Dickey CA. The diarylhep-tanoid (+)-aR,11S-myricanol and two flavones from bayberry (Myrica cerifera) destabilize the microtubule-associated protein tau. J Nat Prod. 2011; 74:38–44. [PubMed: 21141876]
26. Jinwal UK, Koren J 3rd, Borysov SI, Schmid AB, Abisambra JF, Blair LJ, Johnson AG, Jones JR, Shults CL, O'Leary JC 3rd, Jin Y, Buchner J, Cox MB, Dickey CA. The Hsp90 cochaperone, FKBP51, increases Tau stability and polymerizes microtubules. J Neurosci. 2010; 30:591–599. [PubMed: 20071522]
27. Bolte S, Cordelieres FP. A guided tour into subcellular colocalization analysis in light microscopy. J Microsc. 2006; 224:213–232. [PubMed: 17210054]
28. Zhai J, Strom AL, Kilty R, Venkatakrishnan P, White J, Everson WV, Smart EJ, Zhu H. Proteomic characterization of lipid raft proteins in amyotrophic lateral sclerosis mouse spinal cord. FEBS J. 2009; 276:3308–3323. [PubMed: 19438725]
29. Dhar SK, Zhang J, Gal J, Xu Y, Miao L, Lynn BC, Zhu H, Kasarskis EJ, St Clair DK. FUsed in sarcoma is a novel regulator of manganese superoxide dismutase gene transcription. Antioxid Redox Signal. 2014; 20:1550–1566. [PubMed: 23834335]
30. Griffith LM, Pollard TD. The interaction of actin filaments with microtubules and microtubule-associated proteins. J Biol Chem. 1982; 257:9143–9151. [PubMed: 6124545]
31. Li X, Kumar Y, Zempel H, Mandelkow EM, Biernat J, Mandelkow E. Novel diffusion barrier for axonal retention of Tau in neurons and its failure in neurodegeneration. EMBO J. 2011; 30:4825–4837. [PubMed: 22009197]
32. Fulga TA, Elson-Schwab I, Khurana V, Steinhilb ML, Spires TL, Hyman BT, Feany MB. Abnormal bundling and accumulation of F-actin mediates tau-induced neuronal degeneration *in vivo*. Nat Cell Biol. 2007; 9:139–148. [PubMed: 17187063]
33. Braak H, Braak E. Neuropathological stageing of Alzheimer-related changes. Acta Neuropathol. 1991; 82:239–259. [PubMed: 1759558]
34. Braak H, Braak E. Demonstration of amyloid deposits and neurofibrillary changes in whole brain sections. Brain Pathol. 1991; 1:213–216. [PubMed: 1669710]
35. Augustinack J, Schneider A, Mandelkow E-M, Hyman B. Specific tau phosphorylation sites correlate with severity of neuronal cytopathology in Alzheimer's disease. Acta Neuropathol. 2002; 103:26–35. [PubMed: 11837744]
36. Palade GE, Siekevitz P. Liver microsomes; an integrated morphological and biochemical study. J Biophys Biochem Cytol. 1956; 2:171–200. [PubMed: 13319380]
37. Abisambra JF, Scheff S. Brain injury in the context of tauopathies. J Alzheimers Dis. 2014; 40:495–518. [PubMed: 24496078]
38. Benyair R, Ron E, Lederkremer GZ. Protein quality control, retention, and degradation at the endoplasmic reticulum. Int Rev Cell Mol Biol. 2011; 292:197–280. [PubMed: 22078962]
39. McPherson PS, Garcia EP, Slepnev VI, David C, Zhang X, Grabs D, Sossin WS, Bauerfeind R, Nemoto Y, De Camilli P. A presynaptic inositol-5-phosphatase. Nature. 1996; 379:353–357. [PubMed: 8552192]

40. Horowitz PM, Patterson KR, Guillozet-Bongaarts AL, Reynolds MR, Carroll CA, Weintraub ST, Bennett DA, Cryns VL, Berry RW, Binder LI. Early N-terminal changes and caspase-6 cleavage of tau in Alzheimer's disease. J Neurosci. 2004; 24:7895–7902. [PubMed: 15356202]
41. Rissman RA, Poon WW, Blurton-Jones M, Oddo S, Torp R, Vitek MP, LaFerla FM, Rohn TT, Cotman CW. Caspase-cleavage of tau is an early event in Alzheimer disease tangle pathology. J Clin Invest. 2004; 114:121–130. [PubMed: 15232619]
42. Gamblin TC, Chen F, Zambrano A, Abraha A, Lagalwar S, Guillozet AL, Lu M, Fu Y, Garcia-Sierra F, LaPointe N, Miller R, Berry RW, Binder LI, Cryns VL. Caspase cleavage of tau: Linking amyloid and neurofibrillary tangles in Alzheimer's disease. Proc Natl Acad Sci U S A. 2003; 100:10032–10037. [PubMed: 12888622]
43. Rohn TT, Rissman RA, Davis MC, Kim YE, Cotman CW, Head E. Caspase-9 activation and caspase cleavage of tau in the Alzheimer's disease brain. Neurobiol Dis. 2002; 11:341–354. [PubMed: 12505426]
44. Papasozomenos SC. Tau protein immunoreactivity in dementia of the Alzheimer type. I. Morphology, evolution, distribution, and pathogenetic implications. Lab Invest. 1989; 60:123–137. [PubMed: 2492060]
45. Ding Q, Markesbery WR, Chen Q, Li F, Keller JN. Ribosome dysfunction is an early event in Alzheimer's disease. J Neurosci. 2005; 25:9171–9175. [PubMed: 16207876]
46. Pestova TV, Lomakin IB, Lee JH, Choi SK, Dever TE, Hellen CU. The joining of ribosomal subunits in eukaryotes requires eIF5B. Nature. 2000; 403:332–335. [PubMed: 10659855]
47. Strittmatter WJ, Saunders AM, Goedert M, Weisgraber KH, Dong LM, Jakes R, Huang DY, Pericak-Vance M, Schmechel D, Roses AD. Isoform-specific interactions of apolipoprotein E with microtubule-associated protein tau: Implications for Alzheimer disease. Proc Natl Acad Sci U S A. 1994; 91:11183–11186. [PubMed: 7972031]
48. Carlier MF, Simon C, Cassoly R, Pradel LA. Interaction between microtubule-associated protein tau and spectrin. Biochimie. 1984; 66:305–311. [PubMed: 6743699]
49. Higuchi M, Iwata N, Matsuba Y, Takano J, Suemoto T, Maeda J, Ji B, Ono M, Staufenbiel M, Suhara T, Saido TC. Mechanistic involvement of the calpain-calpastatin system in Alzheimer neuropathology. FASEB J. 2012; 26:1204–1217. [PubMed: 22173972]
50. Ringger NC, O'Steen BE, Brabham JG, Silver X, Pineda J, Wang KKW, Hayes RL, Papa L. A novel marker for traumatic brain injury: CSF alphaII-spectrin breakdown product levels. J Neurotrauma. 2004; 21:1443–1456. [PubMed: 15672634]
51. Gauthier-Kemper A, Weissmann C, Golovyashkina N, Sebo-Lemke Z, Drewes G, Gerke V, Heinisch JJ, Brandt R. The frontotemporal dementia mutation R406W blocks tau's interaction with the membrane in an annexin A2-dependent manner. J Cell Biol. 2011; 192:647–661. [PubMed: 21339331]
52. Crary JF, Trojanowski JQ, Schneider JA, Abisambra JF, Abner EL, Alafuzoff I, Arnold SE, Attems J, Beach TG, Bigio EH, Cairns NJ, Dickson DW, Gearing M, Grinberg LT, Hof PR, Hyman BT, Jellinger K, Jicha GA, Kovacs GG, Knopman DS, Kofler J, Kukull WA, Mackenzie IR, Masliah E, McKee A, Montine TJ, Murray ME, Neltner JH, Santa-Maria I, Seeley WW, Serrano-Pozo A, Shelanski ML, Stein T, Takao M, Thal DR, Toledo JB, Troncoso JC, Vonsattel JP, White CL 3rd, Wisniewski T, Woltjer RL, Yamada M, Nelson PT. Primary age-related tauopathy (PART): A common pathology associated with human aging. Acta Neuropathol. 2014; 128:755–766. [PubMed: 25348064]
53. Kim DJ, Martinez-Lemus LA, Davis GE. EB1, p150Glued, and Clasp1 control endothelial tubulogenesis through microtubule assembly, acetylation, and apical polarization. Blood. 2013; 121:3521–3530. [PubMed: 23444400]
54. DuBoff B, Gotz J, Feany MB. Tau promotes neurodegeneration via DRP1 mislocalization *in vivo*. Neuron. 2012; 75:618–632. [PubMed: 22920254]
55. Flanagan LA, Cunningham CC, Chen J, Prestwich GD, Kosik KS, Janmey PA. The structure of divalent cation-induced aggregates of PIP2 and their alteration by gelsolin and tau. Biophys J. 1997; 73:1440–1447. [PubMed: 9284311]

56. Ferhat L, Chevassus au Louis N, Jorquera I, Niquet J, Khrestchatisky M, Ben-Ari Y, Represa A. Transient increase of tenascin-C in immature hippocampus: Astroglial and neuronal expression. J Neurocytol. 1996; 25:53–66. [PubMed: 8852938]
57. Gold MS, Kobeissy FH, Wang KK, Merlo LJ, Bruijnzeel AW, Krasnova IN, Cadet JL. Methamphetamine-and trauma-induced brain injuries: Comparative cellular and molecular neurobiological substrates. Biol Psychiatry. 2009; 66:118–127. [PubMed: 19345341]
58. Song J, Goetz BD, Kirvell SL, Butt AM, Duncan ID. Selective myelin defects in the anterior medullary velum of the taiep mutant rat. Glia. 2001; 33:1–11. [PubMed: 11169787]
59. Avsar T, Korkmaz D, Tutuncu M, Demirci NO, Saip S, Kamasak M, Siva A, Turanli ET. Protein biomarkers for multiple sclerosis: Semi-quantitative analysis of cerebrospinal fluid candidate protein biomarkers in different forms of multiple sclerosis. Mult Scler. 2012; 18:1081–1091. [PubMed: 22252467]
60. Weinger JG, Davies P, Acker CM, Brosnan CF, Tsiperson V, Bayewitz A, Shafit-Zagardo B. Mice devoid of Tau have increased susceptibility to neuronal damage in myelin oligodendrocyte glycoprotein-induced experimental autoimmune encephalomyelitis. J Neuropathol Exp Neurol. 2012; 71:422–433. [PubMed: 22487860]
61. Garver TD, Oyler GA, Harris KA, Polavarapu R, Damuni Z, Lehman RA, Billingsley ML. Tau phosphorylation in brain slices: Pharmacological evidence for convergent effects of protein phosphatases on tau and mitogen-activated protein kinase. Mol Pharmacol. 1995; 47:745–756. [PubMed: 7723735]
62. Jicha GA, Lane E, Vincent I, Otvos L Jr, Hoffmann R, Davies P. A conformation- and phosphorylation-dependent antibody recognizing the paired helical filaments of Alzheimer's disease. J Neurochem. 1997; 69:2087–2095. [PubMed: 9349554]
63. Goedert M, Jakes R, Qi Z, Wang JH, Cohen P. Protein phosphatase 2A is the major enzyme in brain that dephosphorylates tau protein phosphorylated by proline-directed protein kinases or cyclic AMP-dependent protein kinase. J Neurochem. 1995; 65:2804–2807. [PubMed: 7595582]
64. Kimura T, Ono T, Takamatsu J, Yamamoto H, Ikegami K, Kondo A, Hasegawa M, Ihara Y, Miyamoto E, Miyakawa T. Sequential changes of tau-site-specific phosphorylation during development of paired helical filaments. Dementia. 1996; 7:177–181. [PubMed: 8835879]
65. Goedert M, Wischik CM, Crowther RA, Walker JE, Klug A. Cloning and sequencing of the cDNA encoding a core protein of the paired helical filament of Alzheimer disease: Identification as the microtubule-associated protein tau. Proc Natl Acad Sci U S A. 1988; 85:4051–4055. [PubMed: 3131773]
66. Hoffmann R, Lee VM, Leight S, Varga I, Otvos L Jr. Unique Alzheimer's disease paired helical filament specific epitopes involve double phosphorylation at specific sites. Biochemistry. 1997; 36:8114–8124. [PubMed: 9201960]
67. Hashiguchi M, Sobue K, Paudel HK. 14-3-3zeta is an effector of tau protein phosphorylation. J Biol Chem. 2000; 275:25247–25254. [PubMed: 10840038]
68. Chun J, Kwon T, Lee EJ, Kim CH, Han YS, Hong SK, Hyun S, Kang SS. 14-3-3 Protein mediates phosphorylation of microtubule-associated protein tau by serum-and glucocorticoid-induced protein kinase 1. Mol Cells. 2004; 18:360–368. [PubMed: 15650334]
69. Sluchanko NN, Seit-Nebi AS, Gusev NB. Phosphorylation of more than one site is required for tight interaction of human tau protein with 14-3-3zeta. FEBS Lett. 2009; 583:2739–2742. [PubMed: 19647741]
70. Infante AA, Infante D, Chan MC, How PC, Kutschera W, Linhartova I, Mullner EW, Wiche G, Propst F. Ferritin associates with marginal band microtubules. Exp Cell Res. 2007; 313:1602–1614. [PubMed: 17391669]
71. Schmitt-Ulms G, Matenia D, Drewes G, Mandelkow EM. Interactions of MAP/microtubule affinity regulating kinases with the adaptor complex AP-2 of clathrin-coated vesicles. Cell Motil Cytoskeleton. 2009; 66:661–672. [PubMed: 19536824]
72. Talaei F, Van Praag VM, Shishavan MH, Landheer SW, Buikema H, Henning RH. Increased protein aggregation in Zucker diabetic fatty rat brain: Identification of key mechanistic targets and the therapeutic application of hydrogen sulfide. BMC Cell Biol. 2014; 15:1. [PubMed: 24393531]

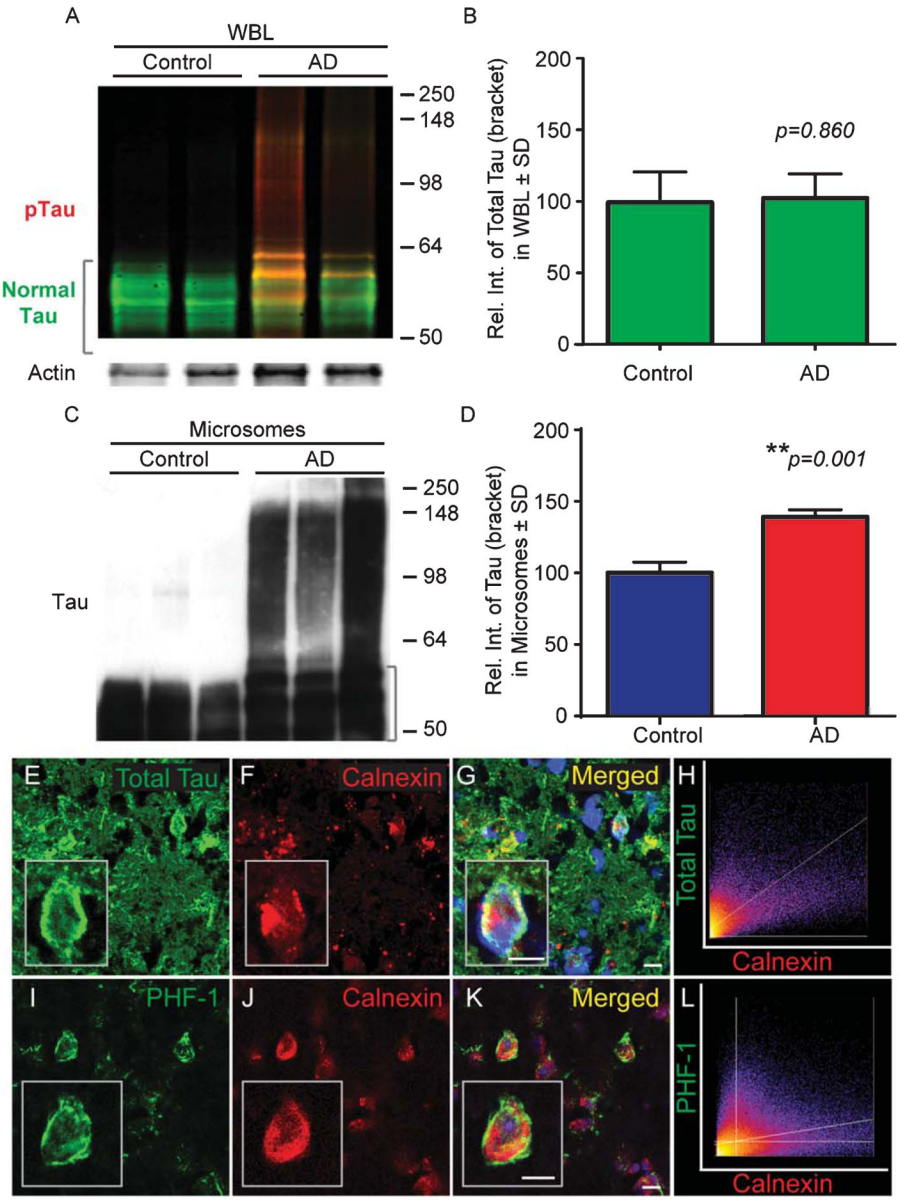

Fig. 1.

Tau is enriched in the endoplasmic reticulum of AD brains. A–D) Representative western blots and quantification analysis (of protein between 48–60kDa) for total tau in whole brain lysate (WBL) (A) or microsomes (C) in human non-demented control and AD brains. Hyperphosphorylated tau (pTau) was detected in the AD samples only (red bands in A). Actin was used as loading control for whole brain lysate. Ponceau S stain before incubation with antibody served as a loading control in the microsome blots. B) Total tau levels are not significantly different in the whole cell lysates of AD and control. D) Tau levels were increased in AD microsomes by 39%. E–L) Representative co-immunofluorescent images of human AD brain showing that both total tau and PHF1-positive signal partially co-localize with calnexin. Sections were stained with antibodies against total tau (green; E and G), PHF1 (green; I and K), and calnexin (red; F, G, J, and K). Cell nuclei were revealed with

DAPI staining (blue). H, L) Co-localization analysis with Manders (avg. 0.79 for total tau and 0.85 for PHF1) and Costes' coefficients reveals that tau partially co-localizes with calnexin. Scale bar = 10 μm.

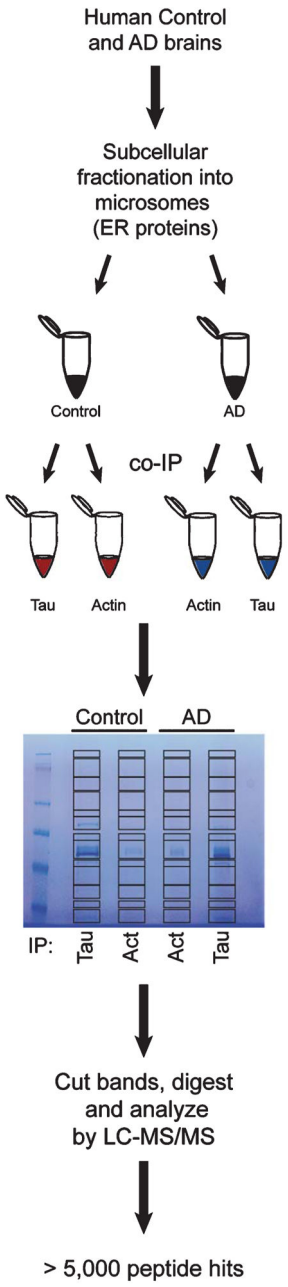

Fig. 2.

Experimental procedure for microsome co-IP-LC-MS/MS. First, microsomes were isolated from AD and non-AD control brains. Then, tau or actin were co-immunoprecipitated from the microsomal protein fractions. Samples were separated by SDS-PAGE, bands were revealed and consequently cut form the gel by Coomassie staining. Sample proteins were trypsinized and subjected to LC-MS/MS.

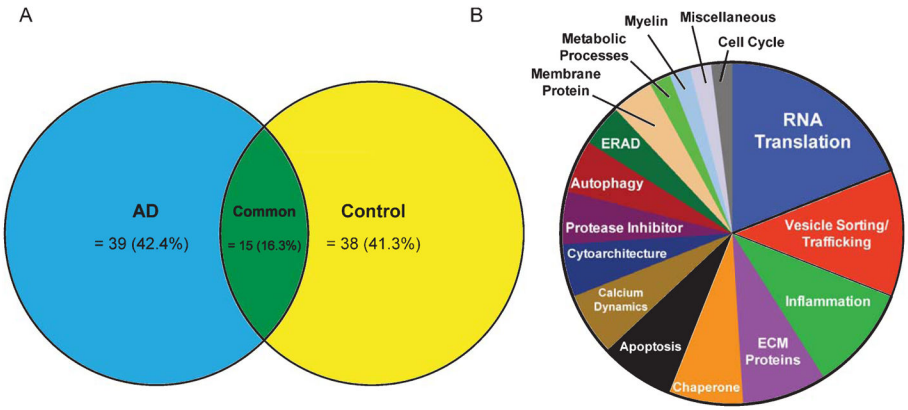

Fig. 3.

Comparison of tau-associated ER proteins in AD and non-AD brains. A) Venn diagram depicting the distribution of tau-associated ER proteins based on tissue of origin. Ninety-two tau-associated ER proteins were identified in AD and non-AD brains. Of these, 39 we only found in AD, 38 were only found in control, and 15 were common between both conditions. B) Pie chart showing the relative abundance of all tau-associated ER proteins identified by function. The identified proteins were grouped into functional categories.

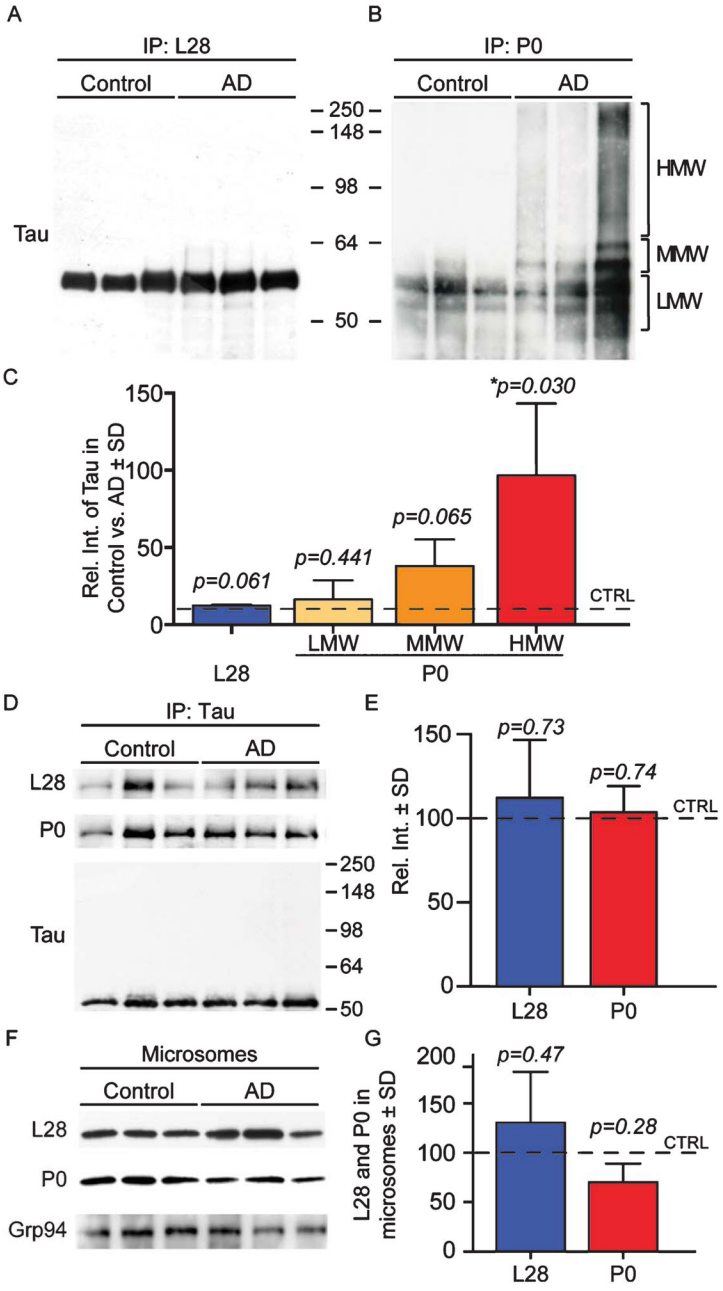

Fig. 4.

Tau associates differentially with L28 and P0 in both AD and control brains. A, B) Representative co-IP-western blots, in which the ribosomal proteins L28 (A) and P0 (B) were co-IP from human control and AD brains. Total tau association with P0 and L28 was determined with western blot with an antibody that recognizes the first 150 aa of tau. C) AD and control samples showed that similar levels of tau co-immunoprecipitated with L28. Tau co-immunoprecipitated more robustly with P0 in the high molecular weight range (HMW) when compared to the medium and low molecular weight bands (MMW and LMW). HMW = 65–250 kDa; MMW = 60–64 kDa; LMW = 50–60 kDa. D) Representative co-IP-western

blot with a tau antibody that recognizes aa 210–241 (Tau5) showed similar co-immunoprecipitation between tau and L28 or P0. E) Quantification of panel D shows that the association of P0 and L28 with Tau 5 is not significantly different. F, G) Representative western blot shows that the levels of L28 and P0 in human control and AD brain microsomes are not statistically significantly different. Grp94 was used as a loading control for microsomes.

Table 1

Tau-associated ER proteins in AD brain only

Accession	Description	Previously described as a tau-associated protein?	Score
Q06033	Inter-alpha-trypsin inhibitor heavy chain H3 OS = Homo sapiens GN = ITIH3 PE = 1 SV = 2 - [ITIH3_HUMAN]	No	203.13
Q9UN36	Protein NDRG2 OS = Homo sapiens GN = NDRG2 PE = 1 SV = 2 - [NDRG2_HUMAN]	No	79.01
Q8IXJ6	NAD-dependent deacetylase sirtuin-2 OS = Homo sapiens GN = SIRT2 PE = 1 SV = 2 - [SIRT2_HUMAN]	Indirect and correlative link with microtubule dynamics [53]	60.57
P27105	Erythrocyte band 7 integral membrane protein OS = Homo sapiens GN = STOM PE = 1 SV = 3 - [STOM_HUMAN]	No	55.41
P08237	6-phosphofructokinase, muscle type OS = Homo sapiens GN = PFKM PE = 1 SV = 2 - [K6PF_HUMAN]	No	54.69
P09525	Annexin A4 OS = Homo sapiens GN = ANXA4 PE = 1 SV = 4 - [ANXA4_HUMAN]	Interacting partner of tau to regulate membrane binding [51]	53.95
P06396	Gelsolin OS = Homo sapiens GN = GSN PE = 1 SV = 1 - [GELS_HUMAN]	No direct interaction; overexpression of gelsolin ameliorates neurodegeneration in tau transgenic mice [54]. Gelsolin and tau bind to PIP2 and have opposing effects on its aggregation [55].	50.52
P19823	Inter-alpha-trypsin inhibitor heavy chain H2 OS = Homo sapiens GN = ITIH2 PE = 1 SV = 2 - [ITIH2_HUMAN]	No	49.60
Q12931	Heat shock protein 75 kDa, mitochondrial OS = Homo sapiens GN = TRAP1 PE = 1 SV = 3 - [TRAP1_HUMAN]	No	45.81
O43813	LanC-like protein 1 OS = Homo sapiens GN = LANCL1 PE = 1 SV = 1 - [LANC1_HUMAN]	No	42.94
P24821	Tenascin OS = Homo sapiens GN = TNC PE = 1 SV = 3 - [TENA_HUMAN]	mRNA for tenascin and tau expressed in the same cells (immature neurons) [56].	42.44
Q13813	Spectrin alpha chain, brain OS = Homo sapiens GN = SPTAN1 PE = 1 SV = 3 - [SPTA2_HUMAN]	Tau interacts with spectrin [48]. Elevated levels in CSF of AD [49] and TBI [50]. Tau and spectrin are subject to cleavage in ischemia [57].	40.35
P23515	Oligodendrocyte-myelin glycoprotein OS = Homo sapiens GN = OMG PE = 1 SV = 2 - [OMGP_HUMAN]	Levels are inversely correlated in *taiep* oligodendrocytes [58]; both increased in CSF of multiple sclerosis clinical subtypes [59]; MOG-induced encephalomyelitis is ameliorated when tau is present [60].	38.81
P05388	60 S acidic ribosomal protein P0 OS = Homo sapiens GN = RPLP0 PE = 1 SV = 1 - [RLA0_HUMAN]	No	37.93
Q8NHW5	60 S acidic ribosomal protein P0-like OS = Homo sapiens GN = RPLP0P6 PE = 5 SV = 1 - [RLA0L_HUMAN]	No	37.93
P01024	Complement C3 OS = Homo sapiens GN = C3 PE = 1 SV = 2 - [CO3_HUMAN]	No	34.67
O75363	Breast carcinoma-amplified sequence 1 OS = Homo sapiens GN = BCAS1 PE = 1 SV = 2 - [BCAS1_HUMAN]	No	34.07
Q13085	Acetyl-CoA carboxylase 1 OS = Homo sapiens GN = ACACA PE = 1 SV = 2 - [ACACA_HUMAN]	No	33.82
P01834	Ig kappa chain C region OS = Homo sapiens GN = IGKC PE = 1 SV = 1 - [IGKC_HUMAN]	No	32.32

Accession	Description	Previously described as a tau-associated protein?	Score
P18583	Protein SON OS = Homo sapiens GN = SON PE = 1 SV = 4 - [SON_HUMAN]	No	31.63
Q9Y696	Chloride intracellular channel protein 4 OS = Homo sapiens GN = CLIC4 PE = 1 SV = 4 - [CLIC4_HUMAN]	No	31.05
Q99683	Mitogen-activated protein kinase kinase kinase 5 OS = Homo sapiens GN = MAP3K5 PE = 1 SV = 1 - [M3K5_HUMAN]	MAPK phosphorylates tau [61] at several sites associated with disease [62–66].	30.63
O75445	Usherin OS = Homo sapiens GN = USH2A PE = 1 SV = 3 - [USH2A_HUMAN]	No	29.78
Q6ZS92	Putative uncharacterized protein FLJ45721 OS = Homo sapiens PE = 5 SV = 2 - [YD022_HUMAN]	No	29.45
P02787	Serotransferrin OS = Homo sapiens GN = TF PE = 1 SV = 3 - [TRFE_HUMAN]	No	29.43
Q9C0B2	Uncharacterized protein KIAA1751 OS = Homo sapiens GN = KIAA1751 PE = 2 SV = 2 - [K1751_HUMAN]	No	29.30
Q16181	Septin-7 OS = Homo sapiens GN = SEPT7 PE = 1 SV = 2 - [SEPT7_HUMAN]	No	28.94
Q8N3Z3	GTP-binding protein 8 OS = Homo sapiens GN = GTPBP8 PE = 2 SV = 1 - [GTPB8_HUMAN]	No	28.86
Q6P5Z2	Serine/threonine-protein kinase N3 OS = Homo sapiens GN = PKN3 PE = 1 SV = 1 - [PKN3_HUMAN]	No	28.65
P37108	Signal recognition particle 14 kDa protein OS = Homo sapiens GN = SRP14 PE = 1 SV = 2 - [SRP14_HUMAN]	No	28.30
Q9NX45	Spermatogenesis- and oogenesis-specific basic helix-loop-helix-containing protein 2 OS = Homo sapiens GN = SOHLH2 PE = 2 SV = 2 - [SOLH2_HUMAN]	No	28.10
P52746	Zinc finger protein 142 OS = Homo sapiens GN = ZNF142 PE = 1 SV = 4 - [ZN142_HUMAN]	No	27.65
P09238	Stromelysin-2 OS = Homo sapiens GN = MMP10 PE = 1 SV = 1 - [MMP10_HUMAN]	No	26.30
Q14624	Inter-alpha-trypsin inhibitor heavy chain H4 OS = Homo sapiens GN = ITIH4 PE = 1 SV = 4 - [ITIH4_HUMAN]	No	26.05
P08195	4F2 cell-surface antigen heavy chain OS = Homo sapiens GN = SLC3A2 PE = 1 SV = 3 - [4F2_HUMAN]	No	25.65
Q9BXR6	Complement factor H-related protein 5 OS = Homo sapiens GN = CFHR5 PE = 1 SV = 1 - [FHR5_HUMAN]	No	25.64
P48643	T-complex protein 1 subunit epsilon OS = Homo sapiens GN = CCT5 PE = 1 SV = 1 - [TCPE_HUMAN]	No	24.40
O43896	Kinesin-like protein KIF1 C OS = Homo sapiens GN = KIF1 C PE = 1 SV = 3 - [KIF1C_HUMAN]	No	24.16
Q8WWZ7	ATP-binding cassette sub-family A member 5 OS = Homo sapiens GN = ABCA5 PE = 2 SV = 2 - [ABCA5_HUMAN]	No	24.10

Table 2

Tau-associated ER proteins in non-demented brain only

Accession	Description	Previously described as a tau-associated protein?	Score
Q04917	14-3-3 protein eta OS = Homo sapiens GN = YWHAH PE = 1 SV = 4 - [1433F_HUMAN]	Yes; particularly studied in relation with zeta subunit of 14-3-3 [67–69]	130.11
Q9Y2J2	Band 4.1-like protein 3 OS = Homo sapiens GN = EPB41L3 PE = 1 SV = 2 - [E41L3_HUMAN]	No	95.21
P31944	Caspase-14 OS = Homo sapiens GN = CASP14 PE = 1 SV = 2 - [CASPE_HUMAN]	No	84.42
Q5D862	Filaggrin-2 OS = Homo sapiens GN = FLG2 PE = 1 SV = 1 - [FILA2_HUMAN]	No	75.88
P06702	Protein S100-A9 OS = Homo sapiens GN = S100A9 PE = 1 SV = 1 - [S10A9_HUMAN]	No	75.56
P05109	Protein S100-A8 OS = Homo sapiens GN = S100A8 PE = 1 SV = 1 - [S10A8_HUMAN]	No	73.36
P09543	2′,3′-cyclic-nucleotide 3′-phosphodiesterase OS = Homo sapiens GN = CNP PE = 1 SV = 2 - [CN37_HUMAN]	No	61.21
O43426	Synaptojanin-1 OS = Homo sapiens GN = SYNJ1 PE = 1 SV = 2 - [SYNJ1_HUMAN]	No	61.16
P61421	V-type proton ATPase subunit d 1 OS = Homo sapiens GN = ATP6V0D1 PE = 1 SV = 1 - [VA0D1_HUMAN]	No	54.66
P31947	14-3-3 protein sigma OS = Homo sapiens GN = SFN PE = 1 SV = 1 - [1433S_HUMAN]	Yes; particularly studied in relation with zeta subunit of 14-3-3 [67–69]	41.58
P02794	Ferritin heavy chain OS = Homo sapiens GN = FTH1 PE = 1 SV = 2 - [FRIH_HUMAN]	Yes. [70]	40.73
Q8N8Y2	V-type proton ATPase subunit d 2 OS = Homo sapiens GN = ATP6V0D2 PE = 2 SV = 1 - [VA0D2_HUMAN]	No	40.48
P60201	Myelin proteolipid protein OS = Homo sapiens GN = PLP1 PE = 1 SV = 2 - [MYPR_HUMAN]	Levels are inversely correlated in *taiep* oligodendrocytes [58]	36.83
O43150	Arf-GAP with SH3 domain, ANK repeat and PH domain-containing protein 2 OS = Homo sapiens GN = ASAP2 PE = 1 SV = 3 - [ASAP2_HUMAN]	No	36.65
Q96A05	V-type proton ATPase subunit E 2 OS = Homo sapiens GN = ATP6V1E2 PE = 1 SV = 1 - [VATE2_HUMAN]	No	35.24
O94973	AP-2 complex subunit alpha-2 OS = Homo sapiens GN = AP2A2 PE = 1 SV = 2 - [AP2A2_HUMAN]	Tau associates with MARK via AP-2 [71]	35.06
Q9NZT1	Calmodulin-like protein 5 OS = Homo sapiens GN = CALML5 PE = 1 SV = 2 - [CALL5_HUMAN]	No	32.84
P17600	Synapsin-1 OS = Homo sapiens GN = SYN1 PE = 1 SV = 3 - [SYN1_HUMAN]	No	32.11
Q12888	Tumor suppressor p53-binding protein 1 OS = Homo sapiens GN = TP53BP1 PE = 1 SV = 2 - [TP53B_HUMAN]	No	30.20
Q6ZP68	Putative uncharacterized protein C13orf35 OS = Homo sapiens GN = C13orf35 PE = 2 SV = 1 - [CM035_HUMAN]	No	30.01
P20930	Filaggrin OS = Homo sapiens GN = FLG PE = 1 SV = 3 - [FILA_HUMAN]	No	29.89
O14594	Neurocan core protein OS = Homo sapiens GN = NCAN PE = 2 SV = 3 - [NCAN_HUMAN]	No	29.82
Q6PJG9	Leucine-rich repeat and fibronectin type-III domain-containing protein 4 OS = Homo sapiens GN = LRFN4 PE = 1 SV = 1 - [LRFN4_HUMAN]	No	28.84
P36957	Dihydrolipoyllysine-residue succinyltransferase component of 2-oxoglutarate dehydrogenase complex, mitochondrial OS = Homo sapiens GN = DLST PE = 1 SV = 3 - [ODO2_HUMAN]	No	28.56
P10915	Hyaluronan and proteoglycan link protein 1 OS = Homo sapiens GN = HAPLN1 PE = 2 SV = 2 - [HPLN1_HUMAN]	No	28.49

Accession	Description	Previously described as a tau-associated protein?	Score
Q92598	Heat shock protein 105 kDa OS = Homo sapiens GN = HSPH1 PE = 1 SV = 1 - [HS105_HUMAN]	No	28.36
Q16658	Fascin OS = Homo sapiens GN = FSCN1 PE = 1 SV = 3 - [FSCN1_HUMAN]	No	28.28
P51674	Neuronal membrane glycoprotein M6-a OS = Homo sapiens GN = GPM6A PE = 1 SV = 2 - [GPM6A_HUMAN]	No	27.75
Q9HCE3	Zinc finger protein 532 OS = Homo sapiens GN = ZNF532 PE = 1 SV = 2 - [ZN532_HUMAN]	No	27.03
P55774	C-C motif chemokine 18 OS = Homo sapiens GN = CCL18 PE = 1 SV = 1 - [CCL18_HUMAN]	No	26.36
Q15334	Lethal(2) giant larvae protein homolog 1 OS = Homo sapiens GN = LLGL1 PE = 1 SV = 3 - [L2GL1_HUMAN]	No	25.52
Q96BH1	E3 ubiquitin-protein ligase RNF25 OS = Homo sapiens GN = RNF25 PE = 1 SV = 1 - [RNF25_HUMAN]	No	25.18
Q9Y2K2	IK3 OS = Homo sapiens GN = SIK3 PE = 1 SV = 3 - [SIK3_HUMAN]	No	23.83
Q6SJ93	Protein FAM111B OS = Homo sapiens GN = FAM111B PE = 2 SV = 1 - [F111B_HUMAN]	No	23.50
O43264	Centromere/kinetochore protein zw10 homolog OS = Homo sapiens GN = ZW10 PE = 1 SV = 3 - [ZW10_HUMAN]	No	23.43
Q9H254	Spectrin beta chain, brain 3 OS = Homo sapiens GN = SPTBN4 PE = 1 SV = 2 - [SPTN4_HUMAN]	No	21.74
Q6N021	Probable methylcytosine dioxygenase TET2 OS = Homo sapiens GN = TET2 PE = 1 SV = 3 - [TET2_HUMAN]	No	20.86
Q9NU22	Midasin OS = Homo sapiens GN = MDN1 PE = 1 SV = 2 - [MDN1_HUMAN]	No	26.11

Table 3

Tau-associated ER proteins common in AD and control brains

Accession	Description	Previously described as a tau-associated protein?	Score
P10636	Microtubule-associated protein tau OS = Homo sapiens GN = MAPT PE = 1 SV = 4 - [TAU_HUMAN]	Yes	721.33
P02751	Fibronectin OS = Homo sapiens GN = FN1 PE = 1 SV = 4 - [FINC_HUMAN]	Fibronectin and tau inclusions are present in Zucker diabetic fatty rat brain [72]	180.85
P68104	Elongation factor 1-alpha 1 OS = Homo sapiens GN = EEF1A1 PE = 1 SV = 1 - [EF1A1_HUMAN]	No	149.33
Q5VTE0	Putative elongation factor 1-alpha-like 3 OS = Homo sapiens GN = EEF1AL3 PE = 5 SV = 1 - [EF1A3_HUMAN]	No	149.33
Q05639	Elongation factor 1-alpha 2 OS = Homo sapiens GN = EEF1A2 PE = 1 SV = 1 - [EF1A2_HUMAN]	No	123.84
P00450	Ceruloplasmin OS = Homo sapiens GN = CP PE = 1 SV = 1 - [CERU_HUMAN]	No	108.22
Q9UK22	F-box only protein 2 OS = Homo sapiens GN = FBXO2 PE = 1 SV = 2 - [FBX2_HUMAN]	No	51.26
P00738	Haptoglobin OS = Homo sapiens GN = HP PE = 1 SV = 1 - [HPT_HUMAN]	No	47.95
P20742	Pregnancy zone protein OS = Homo sapiens GN = PZP PE = 1 SV = 4 - [PZP_HUMAN]	No	41.12
P01023	Alpha-2-macroglobulin OS = Homo sapiens GN = A2M PE = 1 SV = 3 - [A2MG_HUMAN]	No	41.12
Q92985	Interferon regulatory factor 7 OS = Homo sapiens GN = IRF7 PE = 1 SV = 2 - [IRF7_HUMAN]	No	33.87
P31946	14-3-3 protein beta/alpha OS = Homo sapiens GN = YWHAB PE = 1 SV = 3 - [1433B_HUMAN]	No	32.98
P46779	60 S ribosomal protein L28 OS = Homo sapiens GN = RPL28 PE = 1 SV = 3 - [RL28_HUMAN]	No	27.67
P02649	Apolipoprotein E OS = Homo sapiens GN = APOE PE = 1 SV = 1 - [APOE_HUMAN]	Yes [47]	24.52
Q6ZQQ6	WD repeat-containing protein 87 OS = Homo sapiens GN = WDR87 PE = 2 SV = 3 - [WDR87_HUMAN]	No	24.26